Materials Research Proceedings 44 (2024) 2-10 https://doi.org/10.21741/9781644903254-1

Microstructure and hot deformation behavior of twin roll cast ZAX210 magnesium wire

KADEN Christoph[1,a *], GHORPADE Vishal[1,b], ULLMANN Madlen[1,c] and PRAHL Ulrich[1,d]

[1]Institute of Metal Forming, Technische Universität Bergakademie Freiberg, Bernhard-von-Cotta-Straße 4, 09599 Freiberg, Germany

[a]christoph.kaden@imf.tu-freiberg.de, [b]vishal.ghorpade@student.tu-freiberg.de, [c]madlen.ullmann@imf.tu-freiberg.de, [d]ulrich.prahl@imf.tu-freiberg.de

Keywords: Twin-Roll Casting, Mg-2Zn-1Al-0.3Ca, Flow Curve, Processing Map

Abstract. The hot deformation behavior of a Mg-2Zn-1Al-0.3Ca (ZAX210) wire, manufactured by twin roll casting was investigated by hot compression tests conducted at different temperatures (250 – 400°C) and strain rates (0.01 - 10 s^{-1}). The analyses of the microstructure and the texture are determined by an optical microscope and scanning electron microscope. A processing map is developed to identify optimal process parameters. The twin roll cast state shows the presence of $\{10\bar{1}2\}$ extension twins, $\{10\bar{1}1\}$ compression twins, double twins, and a weak prismatic texture. Furthermore, regions with small recrystallized grains as well as a small segregation line extend across the center of the wire. The heat treatment at 420°C for 2 h results in a grain structure, consisting of equiaxed grains with an average grain size of approximately 32 µm in the center and 17 µm at the edges of the wire. The heat treatment further reduces the segregation and weakens the texture by spreading the basal plane along the transverse direction. In contrast to the initial state, only $\{10\bar{1}2\}$ extension twins can be observed. The experimental results of the compression tests show that the flow stress increases with higher strain rates and decreasing temperatures. The course of the flow curves indicate that dynamic recrystallization occurs during hot deformation. The activation energy for plastic deformation of the twin roll cast and heat-treated wire is calculated to 150 kJ/mol. The process map identifies optimal process parameters, while deviations from these parameters result in crack formation, primarily at grain boundaries.

Introduction

As the lightest engineered metal, Magnesium and its alloys have garnered significant attention in the last decades. The low density, high strength-to-weight ratio and good castability make it an appealing choice across various industries, ranging from automotive [1] and aerospace [2] to biomedical applications [1,3]. However, the use of magnesium alloys is limited by their poor formability at room temperature due to inadequate slip systems. There are several methods to improve formability by achieve grain refinement and texture modification. One approach is to add rare earth elements as alloying elements [4,5]. A more cost-effective alternative is the use of calcium as an alloying element [6]. In addition to improving formability at room temperature, calcium improves corrosion resistance [7] and strength at elevated temperatures [8]. In the field of additive manufacturing, magnesium wires are particularly important as they are also used to weld components [9]. The conventional method of manufacturing magnesium wires involves casting followed by multiple extrusions with intermediate heat treatments [10]. However, this approach has drawbacks such as multiple process steps and length limitations. A cost and energy saving alternative is the combination of twin-roll casting and wire rolling [11]. By combining the casting and rolling processes, semi-finished products with near-net-shape geometry can be produced in a single step using the twin-roll casting process. The chosen process parameters for the subsequent wire rolling process are critical, making the study of the hot forming behavior of magnesium alloys

of great interest. Kittner et al. [12] determined an activation energy of 180.5 kJ/mol for twin-roll cast strips of the alloy ZAX210. Temperatures above 370 °C and strain rates between 3 s^{-1} and 10 s^{-1} led to instabilities. For twin-roll cast wire, Arndt et al. [13] determined an activation energy of 159.0 kJ/mol and an instability range for temperatures between 250 °C and 375 °C and strain rates between 0.01 s^{-1} and 10 s^{-1} for the alloy AZ31. The present study focuses on the microstructural investigation and hot forming behavior of twin-roll cast and heat treated ZAX210 alloy wires. Based on the obtained stress-strain curves and microstructural observations, process maps were developed to derive optimum parameters for hot forming of the ZAX210 alloy.

Material and Methods

The investigated wire was produced at the twin-roll casting plant of the Institute for Metal Forming at the TU Bergakademie Freiberg [14]. In this process, magnesium ingots were melted in a furnace and fed through a heated nozzle at a temperature of 690°C into the rolling gap between two rotating, water-cooled rolls. Upon contact with the rolls, the melt begins to solidify from the outside inward and undergoes initial deformation. The chemical composition of the magnesium ingots used is shown in Table 1. The casting speed is 4.0 m/min, the oval cross-section of the twin-roll cast wire is 20 mm x 9.2 mm.

Table 1: Chemical composition of the ZAX210 alloy (wt.%).

Zn	Al	Ca	Mn	Fe	Ni	Cu	Mg
2.000	0.741	>0.180	0.037	0.006	0.003	0.001	Bal.

Heat treatment was carried out according to previous studies at 420°C for 2 hours [12]. The samples were placed in a preheated furnace and quenched in water (room temperature) after the holding time. Compression test specimens with a diameter of 5 mm and a height of 10 mm were then machined from the heat-treated specimens. Compression tests were performed using a BÄHR DIL 805 D quenching and deformation dilatometer at temperatures of 250, 300, 350, and 400°C and strain rates of 0.01, 0.1, 1, and 10 s^{-1} up to an equivalent logarithmic strain of 1. First, the samples were heated to the deformation temperature at a heating rate of 5 K/s. To ensure a uniform temperature throughout the sample volume, the temperature was held for 5 minutes. To preserve the deformed microstructure, the samples were quenched at a cooling rate of 100 K/s after forming. After data acquisition, stress-strain curves were determined and corrected for temperature and friction. For microstructural studies, the samples were sectioned, ground with silicon carbide paper, polished with OPS, and finally etched with a solution of ethanol, acetic acid, picric acid, and distilled water. The microstructure of the longitudinal section of the sample was examined using a Keyence VHX-6000 optical microscope and a ZEISS GeminiSEM 450 scanning electron microscope. Texture measurements were performed using an electron backscatter diffraction (EBSD) detector.

The developing of the processing map is based on the dynamic materials model (DMM) [15]. The processing map is a superimposition of a power dissipation and an instability map and represents the response of a material to the given process parameters. During a forming process, the total power P dissipates in the generation of heat (G content) and in microstructural changes (J co-content). The relationship can be expressed as follows:

$$P = G + J = \int_0^{\dot{\varepsilon}} \sigma d\dot{\varepsilon} + \int_0^{\sigma} \dot{\varepsilon} d\sigma \ . \quad (1)$$

The efficiency of power dissipation (η) represents the power dissipation used for microstructural changes and is described as follows:

$$\eta = \frac{2 \cdot m}{m + 1} \quad , \tag{2}$$

where m is the strain rate sensitivity. To obtain the power dissipation map, the efficiency parameter is plotted as a function of temperature and strain rate. The instability map can be obtained with the instability parameter ($\xi(\dot{\varepsilon})$), given by:

$$\xi(\dot{\varepsilon}) = \frac{\partial \ln\left(\frac{m}{m+1}\right)}{\partial \ln \dot{\varepsilon}} + m \leq 0 \quad . \tag{3}$$

When the value of $\xi(\dot{\varepsilon})$ is negative, metallurgical instability during plastic flow occurs.

Results and Discussion

Microstructure of Twin-Roll Cast and Heat-Treated Alloy. The initial state for the subsequent investigations is the twin-roll cast and heat-treated condition. Fig. 1a shows the corresponding microstructure. The already minimal centerline segregation after twin-roll casting was completely reduced by the heat treatment. In addition, globular grains have formed. At the upper edge, the average grain size is 17 µm (19 µm at the lower edge). In the center, there is a larger grain size distribution with an average grain size of 32 µm (Fig. 2). The chemical composition of individual regions can be determined by EDX measurements (Fig. 1b, c). After heat treatment, the precipitates are relatively finely distributed within the Mg solid solution, especially at the edges. The precipitates contain high amounts of Zn and almost equal amounts of Al and Ca. According to Katsarou et al [16], these are most likely the $Mg_6Ca_2Zn_3$ phase. Furthermore, twins can be observed in the microstructure. The misorientation distribution (Figure 1d) shows a distinct peak between 85 and 90 degrees, caused by $\{10\bar{1}2\}$ extension twins. There is no obvious preferred orientation from the pole figures. The intensity maxima are distributed along the transverse direction and are weakly pronounced (Fig. 3).

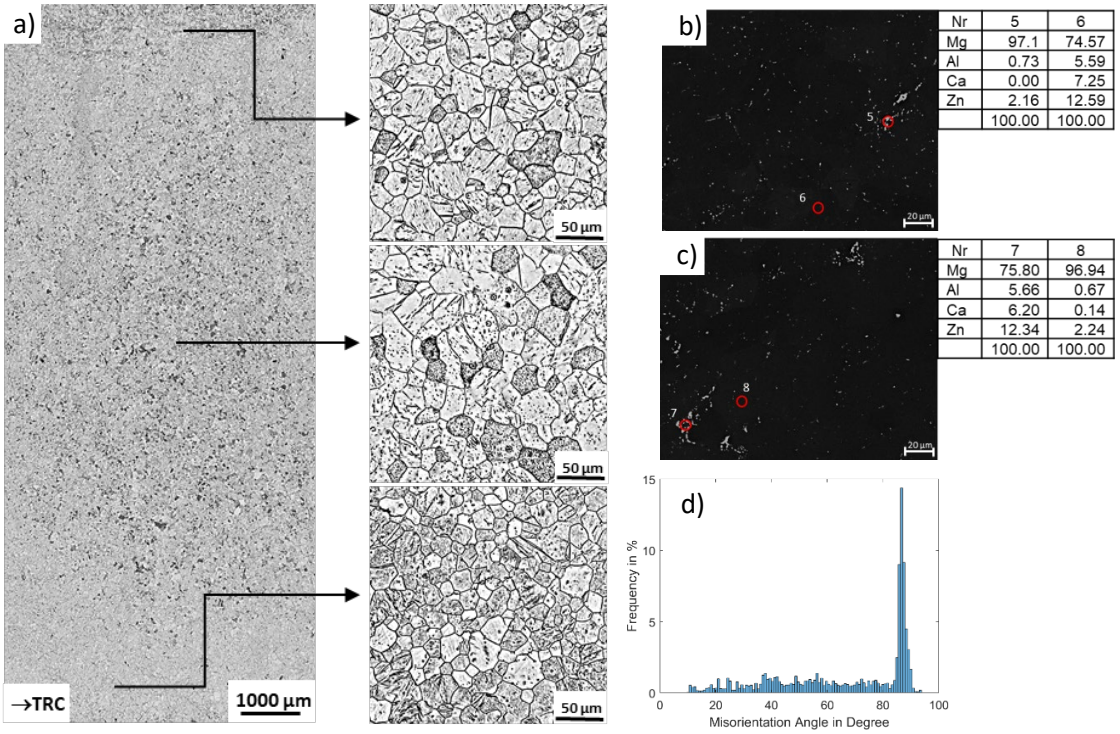

Fig. 1. (a) Microstructure of the twin-roll cast and annealed (420°C, 2 h) ZAX210 alloy in longitudinal view, EDS measurement of the (b) edge and (c) middle of the wire and (d) misorientation angle distribution.

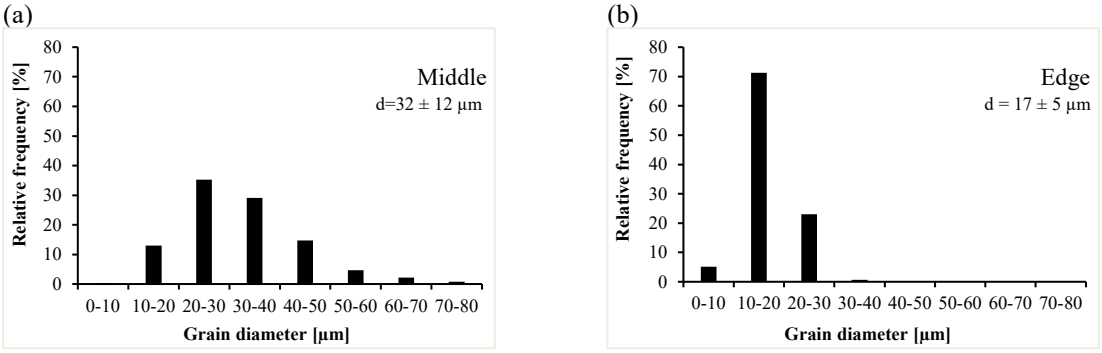

Fig. 2. Grain size distribution of the twin-roll cast and heat-treated (420°C, 2 h) ZAX210 alloy, (a) wire center and (b) upper edge area.

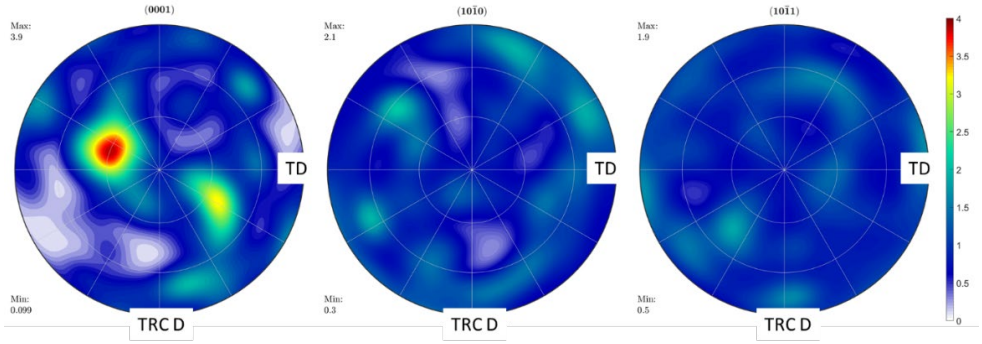

Fig. 3. (0001)-basal, (10$\bar{1}$0)-prismatic and (10$\bar{1}$1)-pyramidal pole figures of the twin-roll cast and annealed (420°C, 2 h) ZAX210 alloy of wire center calculated from electron backscatter diffraction (EBSD).

Flow Behavior. Fig. 4 shows the stress-strain curves of the twin-roll cast and heat-treated ZAX210 alloy at temperatures ranging from 250°C to 400°C and strain rates of 0.01 s^{-1}, 0.1 s^{-1}, 1 s^{-1}, and 10 s^{-1}. The curves demonstrate that the flow behavior, i.e., strain hardening and softening, is influenced by both temperature and strain rate. At the onset of deformation, strain hardening takes place, which is marked by an increase in dislocation density. This leads to a rapid rise in the stress-strain curve at low degrees of deformation. The flow stress increases as the strain rate increases and the temperature decreases, indicating strain hardening. Furthermore, the peak flow stress increases at higher equivalent strain values due to the greater dislocation multiplication at higher strain rates. This leads to dislocations obstructing each other, resulting in an increase in flow stress. Additionally, there is insufficient time for diffusion-controlled softening processes to occur. The flow stress decreases with increasing temperature or decreasing strain rate due to slower dislocation multiplication, longer duration for dynamic recrystallization, and enhanced diffusion at higher temperatures. Furthermore, the critical resolved shear stress (CRSS) for non-basal slip systems decreases with increasing temperature. At high temperatures and low strain rates (400°C, 0.01 s^{-1}), there is only a slight increase in the stress-strain curve, resulting in minimal strain hardening. Once the maximum flow stress is reached, the curve decreases due to softening mechanisms such as dynamic recrystallization. However, a significant decrease in flow stress is only observed at 350°C and 400°C and 10 s^{-1}. At other deformation parameters, the stress-strain curve remains nearly constant. Additionally, the effect of strain rate on flow stress appears to be dependent on temperature. At 250°C, the strain rate (excluding 0.01 s^{-1}) has minimal impact on flow stress, but its influence becomes more significant as the temperature increases. This observation aligns with Rao's findings for the calcium-containing alloy ZX11 [17].

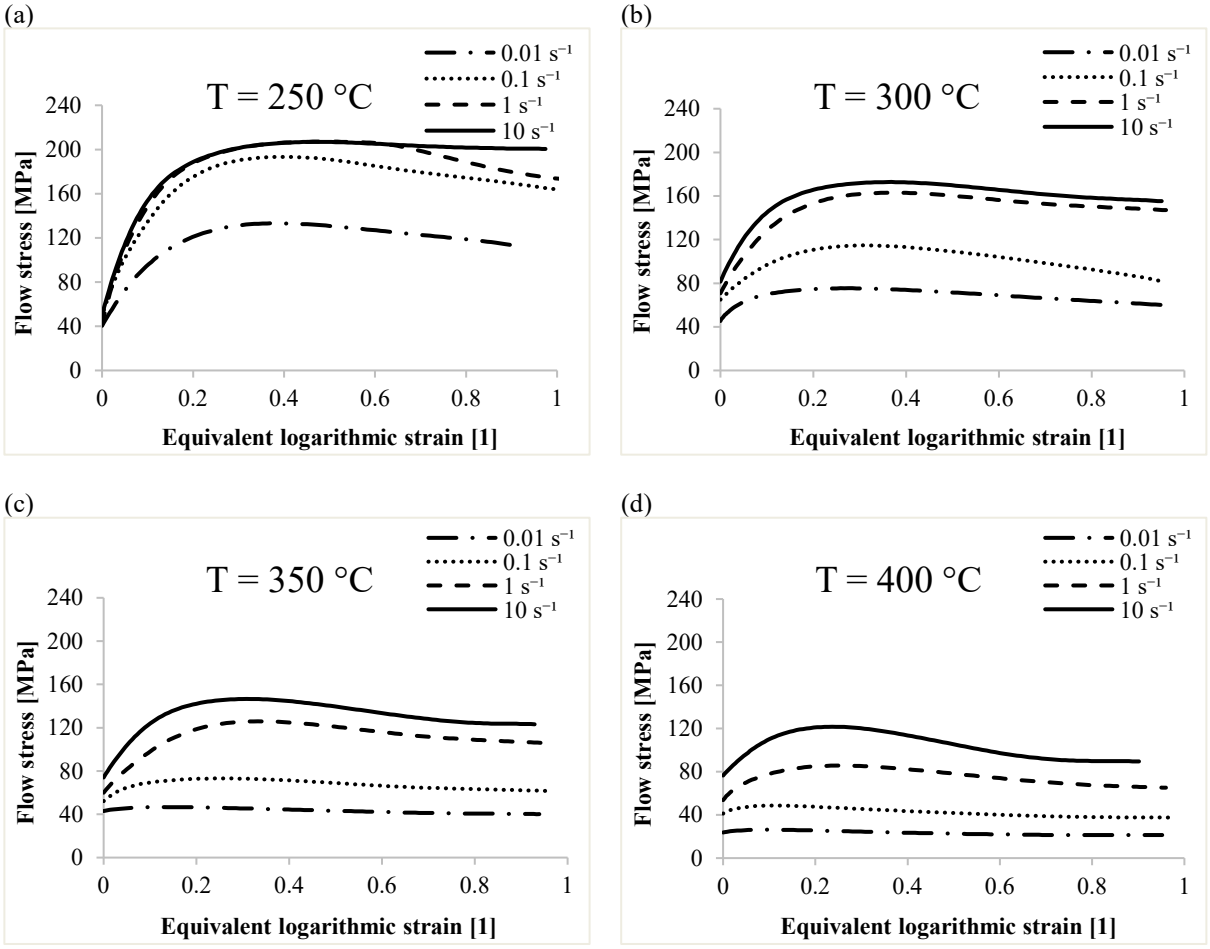

Fig. 4. Flow curves of the twin-roll cast and heat-treated ZAX210 alloy at different forming speeds and temperatures: (a) 250°C, (b) 300°C, (c) 350°C and (d) 400°C.

Analysis of Hot Deformation Behavior of Twin-Roll Cast and Heat-Treated ZAX210 Alloy. As shown in the stress-strain curves, the flow behavior depends on temperature, strain rate, and degree of deformation. The relationships between flow stress and deformation parameters can be described using the Arrhenius equations, developed by Sellars and Tegart [18]. The relationship, valid for all stress conditions, is expressed as:

$$\dot{\varepsilon}=A\,[\sinh(\alpha\sigma)]^{n}\exp\left(-\frac{Q}{RT}\right)\ , \tag{4}$$

Where $\dot{\varepsilon}$ is the strain rate (s^{-1}), A is a material constant, n is the stress exponent, α is a fitting parameter (MPa^{-1}), Q represents the activation energy for plastic flow (kJ/mol), σ is the peak flow stress (MPa), R is the gas constant (8.314 J/(mol·K)), and T signifies the deformation temperature (K). Utilizing the mean values obtained from the slopes of the graphs depicting the linear dependency among flow stress, strain rate, and temperature, the parameters can be determined. Accordingly, the following values are obtained: $A = 6.62585 \times 10^{12}\ s^{-1}$, n = 7.335, $\alpha = 0.0092\ MPa^{-1}$, and Q = 149.68 kJ/mol. These determined parameters are valid for temperatures ranging from 250°C to 400°C and strain rates from 0.01 s^{-1} to 10 s^{-1}. The activation energy Q serves as an indicator of the difficulty in initiating deformations during hot forming. The calculated value exceeds the lattice diffusion of magnesium (135 kJ/mol). The high value of Q can be attributed to the fine microstructure and the presence of precipitates. Small grains lead to more grain boundaries, which hinder the movement of dislocations. Likewise, precipitates lead to an obstruction of dislocation movement, making self-diffusion more difficult [12,19].

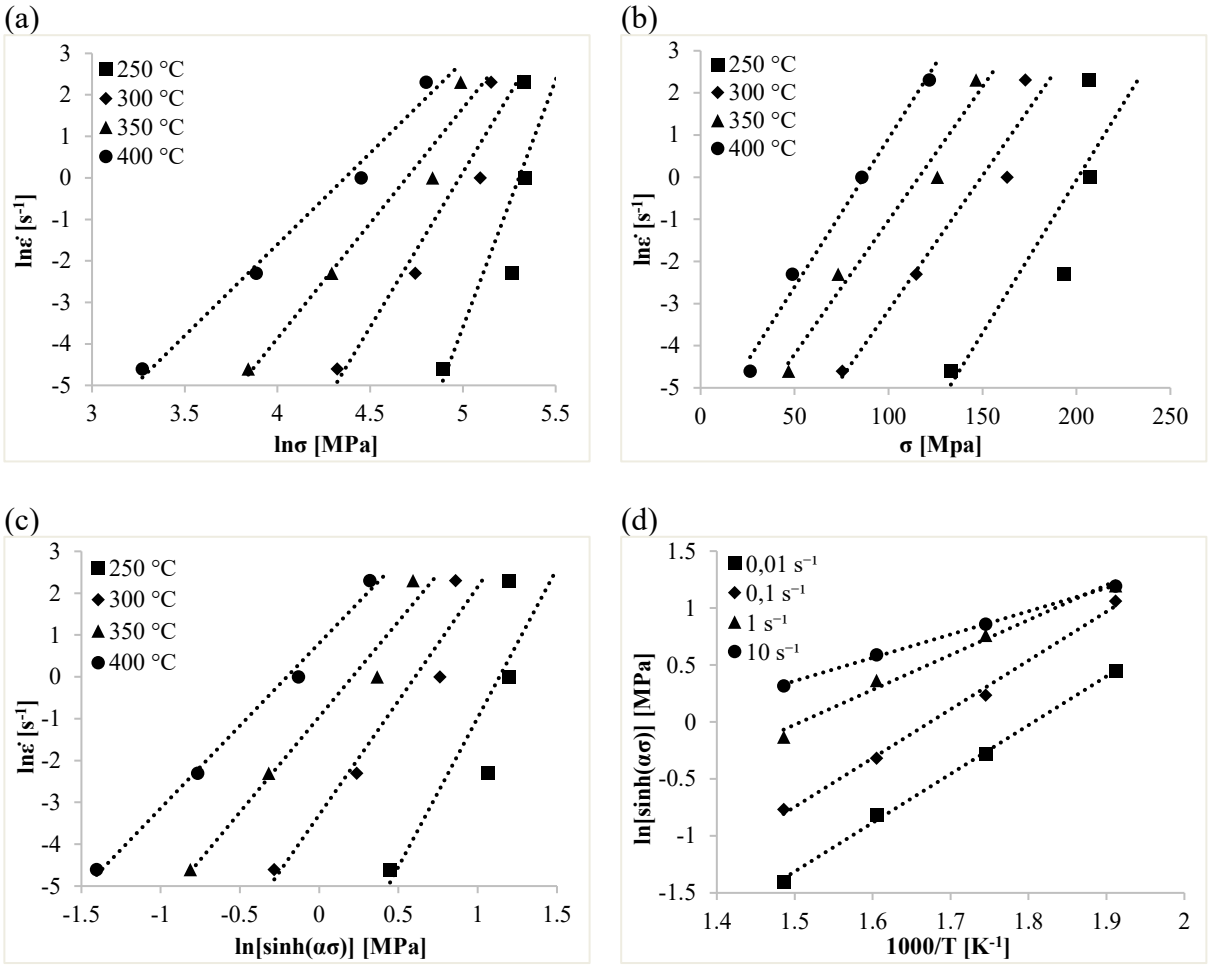

Fig. 5. Relationship between ln(ε) and (a) lnσ and (b) σ as a function of the forming temperature as well as (c) ln(ε) and ln[sinh(ασ)] at different forming temperatures and (d) $ln[sinh(\alpha\sigma)]^{-1}/T$ as a function of the strain rate.

To describe the the influence of temperature and strain rate on the material flow behavior, the Zener-Hollomon parameter Z is employed. Taking Eq. 4 into account, the following formula is derived for the calculation of Z:

$$Z=\dot{\varepsilon}\exp\left(\frac{Q}{RT}\right)=A\,[\sinh(\alpha\sigma)]^{n}. \quad (5)$$

The linear relationship between ln Z and ln[sinh(ασ)] is depicted in Fig. 6. The linear regression was determined with an accuracy of (R^2) = 0.94. According to Eq. 5, the stress exponent n can be calculated to 5.01. This value can be utilized to estimate the dominant mechanism of plastic flow. Dislocation climb creep is cited in the literature as the deformation mechanism for a stress exponent ranging between 4 and 6 [20].

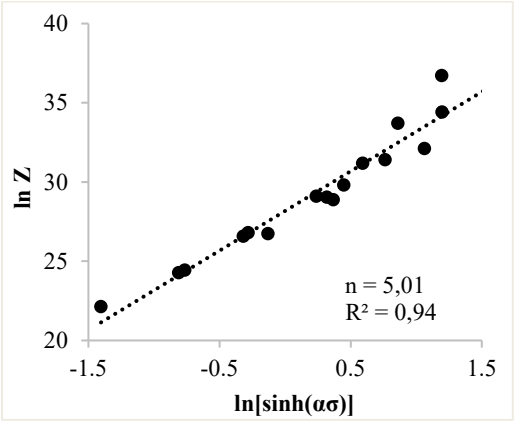

Fig. 6. Relationship between ln Z and ln[sinh(ασ)].

Processing Map. The process map for the twin-roll cast and heat-treated ZAX210 wire is shown in Fig. 7a. It is valid for an equivalent logarithmic strain of 0.4, as it reflects a typical rolling pass. The numbers along the contour lines correspond to the power dissipation efficiency η. The gray shaded area indicates the instability range. This range is observed at temperatures between 250°C and 350°C, with strain rates ranging from 0.14 s^{-1} to 1.8 s^{-1}. For temperatures above 350°C, the range shifts to strain rates of 1 s^{-1} to 10 s^{-1}. Under these conditions, crack formation occurs, preferably along grain boundaries (Fig. 7b). In contrast, Fig. 7c displays a crack-free microstructure with dynamic recrystallization at grain boundaries and twin boundaries. Under these parameters, hot forming is feasible without issues. The instability at 400°C and high strain rates also aligns with the findings of Kittner et al. [12] for strip material.

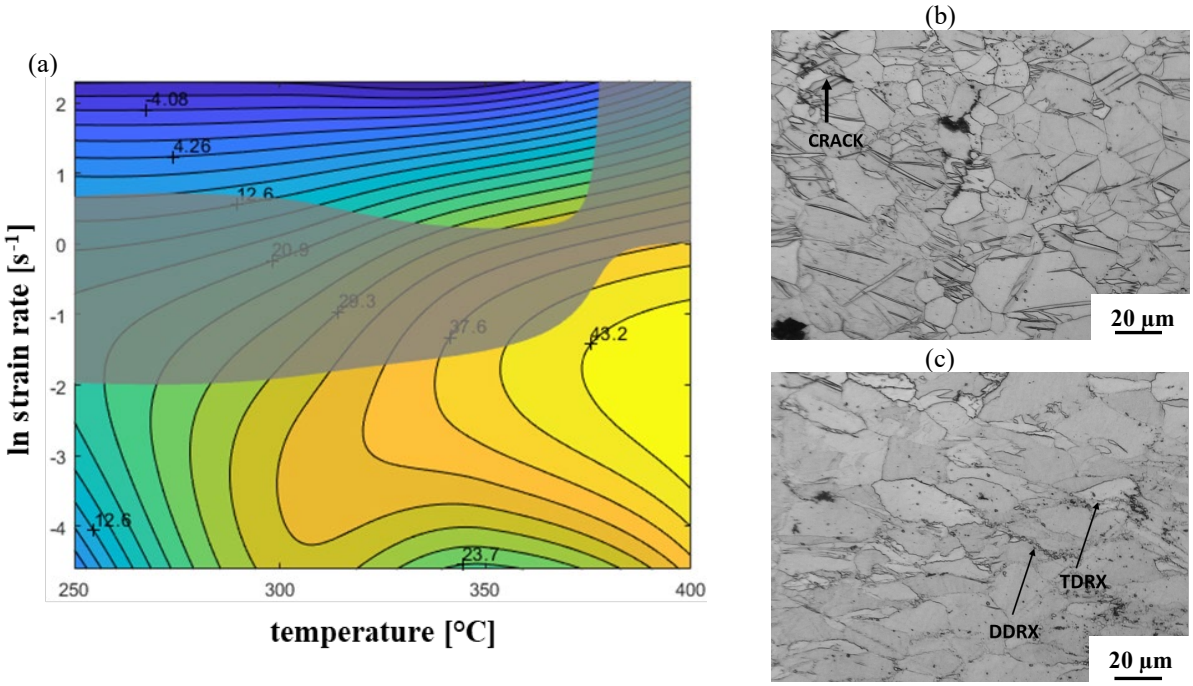

Fig. 7. (a) Processing Map of the twin-roll cast and annealed (420°C, 2 h) ZAX210 alloy at an equivalent strain of 0.4, (b) microstructure within the instability domain (400°C; 10 s^{-1}) and (c) resulting microstructure in stable domain (350°C; 0.1 s^{-1}).

Conclusions

In this study, to hot forming behavior of a twin-roll cast and heat-treated wire of the ZAX210 alloy was investigated. The following conclusions can be drawn:

(1) The determined stress-strain curves exhibit a typical behavior, with the flow stress

increasing with increasing strain rate or decreasing temperature.

(2) Using the Arrhenius equation, an activation energy for plastic deformation of 150 kJ/mol was determined.

(3) The stress exponent of 5.01 suggests dislocation climb creep as the dominant deformation mechanism.

(4) The process map for an equivalent logarithmic strain of 0.4 shows an instability range from 0.14 s^{-1} to 1.8 s^{-1} for temperatures ranging from 250 °C to 350 °C. Above 350 °C, the range shifts from 1 s^{-1} to 10 s^{-1}. Particularly at high temperatures and high strain rates, cracks propagate along grain boundaries.

Funding

The authors would like to thank the Federal Ministry for Economic Affairs and Climate Action for supporting this research work through the project “CLEAN-Mag: CO2-neutral production of lightweight magnesium components”, project no. 03LB3080A, part of the Technologietransfer-Programm Leichtbau (TTP LB).

References

[1] B. Liu, J. Yang, X. Zhang, Q. Yang, J. Zhang, X. Li, Development and application of magnesium alloy parts for automotive OEMs: A review, J. Magnes. Alloy. 11 (2023) 15–47. https://doi.org/10.1016/j.jma.2022.12.015

[2] J. Bai, Y. Yang, C. Wen, J. Chen, G. Zhou, B. Jiang, X. Peng, F. Pan, Applications of magnesium alloys for aerospace: A review, J. Magnes. Alloy. 11 (2023) 3609–3619. https://doi.org/10.1016/j.jma.2023.09.015

[3] T. Zhang, W. Wang, J. Liu, L. Wang, Y. Tang, A review on magnesium alloys for biomedical applications, Frontiers in Bioengineering and Biotechnology (2022). https://doi.org/10.3389/fbioe.2022.953344

[4] L. M. Calado, M. J. Carmezim, F. Montemor, Rare Earth Based Magnesium Alloys - A Review on WE Series, Frontiers in Materials (2022). https://doi.org/10.3389/fmats.2021.804906

[5] H. Cai, Z. Wang, L. Liu, J. Su, Y. Li, F. Guo, Grain Refinement Mechanism of Rare Earth Elements (Ce, Y and Gd) on AZ91 Magnesium Alloy at Different Cooling Rates, Inter Metalcast (2023). https://doi.org/10.1007/s40962-023-01204-5

[6] Y. Li, B. Liu, J. Wang, Y. Sun, H. Li, Effect of Rare Earth and Ca Micro-Alloying on the Microstructure and Anisotropy of AZ31 Magnesium Alloy Sheets, Metals 12 (2022) 1724. https://doi.org/10.3390/met12101724

[7] D. Wan, Y. Wang, S. Dong, Y. Xue, G. Han, F. Yang, H. Tang, J. Kang, G. Zeng, J. Xu, Improving corrosion resistance of high strength Mg-Zn-Y alloy through Ca addition, Corrosion Engineering, Science and Technology 57 (2022) 789–795. https://doi.org/10.1080/1478422X.2022.2127637

[8] C. Hou, F. Qi, L. Wang, L. Lu, N. Zhao, J. She, Y. Zhou, X. Ouyang, Effects of Ca addition on the microstructure and mechanical properties of Mg–Zn–Sn–Mn alloys, J. Mater. Res. Technol. 25 (2023) 3884–3900. https://doi.org/10.1016/j.jmrt.2023.06.194

[9] S.K. Manjhi, P. Sekar, S. Bontha, A. Balan, Additive manufacturing of magnesium alloys: Characterization and post-processing, Int. J. Lightweight Mater. Manuf. 7 (2024) 184–213. https://doi.org/10.1016/j.ijlmm.2023.06.004

[10] M. Nienaber, M. Braatz, N. Ben Khalifa, J. Bohlen, Property profile development during wire extrusion and wire drawing of magnesium alloys AZ31 and ZX10, Materials & Design 224 (2022) 111355. https://doi.org/10.1016/j.matdes.2022.111355

[11] M. Moses, M. Ullmann, R. Kawalla, U. Prahl, Improving Mechanical Properties of Twin-Roll Cast AZ31 by Wire Rolling, MSF 1016 (2021) 957–963. https://doi.org/10.4028/www.scientific.net/MSF.1016.957

[12] K. Kittner, M. Ullmann, T. Henseler, R. Kawalla, U. Prahl, Microstructure and Hot Deformation Behavior of Twin Roll Cast Mg-2Zn-1Al-0.3Ca Alloy, Materials (Basel, Switzerland) 12 (2019). https://doi.org/10.3390/ma12071020

[13] F. Arndt, S. Berndorf, M. Moses, M. Ullmann, U. Prahl, Microstructure and Hot Deformation Behaviour of Twin-Roll Cast AZ31 Magnesium Wire, Crystals 12 (2022) 173. https://doi.org/10.3390/cryst12020173

[14] Marie Moses, Twin Roll Casting of Magnesium Wire: An Innovative Continuous Production Route, Frontiers in Bioengineering and Biotechnology. https://doi.org/10.37904/metal.2019.812

[15] Y.V.R.K. Prasad, K.P. Rao, S. Sasidhara, Hot Working Guide. A Compendium of Processing Maps, ASM International (2015).

[16] L. Katsarou, K. Suresh, K.P. Rao, N. Hort, C. Blawert, C.L. Mendis, H. Dieringa, Microstructure and Properties of Magnesium Alloy Mg-1Zn-1Ca (ZX11), Magnesium Technol. (2015). https://doi.org/10.1007/978-3-319-48185-2_78

[17] K. Rao, K. Suresh, Y. Prasad, C. Dharmendra, N. Hort, H. Dieringa, High Temperature Strength and Hot Working Technology for As-Cast Mg–1Zn–1Ca (ZX11) Alloy, Metals 7 (2017) 405. https://doi.org/10.3390/met7100405

[18] C.M. Sellars, W.J. McTegart, On the mechanism of hot deformation, Acta Metall. 14 (1966) 1136–1138. https://doi.org/10.1016/0001-6160(66)90207-0

[19] J. Qi, Y. Du, B. Jiang, M. Shen, Hot deformation behavior and microstructural evolution of Mg–Zn–Ca–La alloys, J. Mater. Res. 33 (2018) 2817–2826. https://doi.org/10.1557/jmr.2018.265

[20] C. Zhaoyun, T. Rui, D. Zichao, Plastic Flow Characteristics of an Extruded Mg-Li-Zn-RE Alloy, Rare Metal Mater. Eng. 42 (2013) 1779–1784. https://doi.org/10.1016/S1875-5372(14)60004-7